

# LARGE-SCALE OPEN-CHANNEL EXPERIMENTS ON THE COLLAPSE OF ABUTMENT BACKFILL OWING TO FLOODS AND PROPOSED COUNTERMEASURE

Shunzo KAWAJIRI<sup>1</sup>, Kohei ONMAYASHIKI<sup>2</sup>, Yasuharu WATANABE<sup>3</sup>,  
Tomoya MATSUDA<sup>4</sup>, Masaki KOYAMA<sup>5</sup>, Yasunori MIYAMORI<sup>6</sup>  
and Takayuki KAWAGUCHI<sup>7</sup>

<sup>1</sup>Member of JSCE, Associate Professor, Faculty of Engineering, Kitami Institute of Technology  
(165 Koen-cho Kitami, Hokkaido 090-8507, Japan)

E-mail: skawajiri@mail.kitami-it.ac.jp (Corresponding Author)

<sup>2</sup>Member of JSCE, Geotechnical Research Team, Civil Engineering Research Institute for Cold Regions,  
Public Works Research Institute (1-34 Hiragishi 1-jo 3-chome, Toyohira-ku, Sapporo, Hokkaido 062-8602, Japan)

E-mail: onmayashiki-k@ceri.go.jp

<sup>3</sup>Member of JSCE, Professor, Faculty of Engineering, Kitami Institute of Technology  
(165 Koen-cho Kitami, Hokkaido 090-8507, Japan)

E-mail: y-watanb@mail.kitami-it.ac.jp

<sup>4</sup>Student Member of JSCE, Graduate School of Engineering, Kitami Institute of Technology (ditto)

E-mail: m1952200210@std.kitami-it.ac.jp

<sup>5</sup>Student Member of JSCE, Graduate School of Engineering, Kitami Institute of Technology (ditto)

E-mail: m2052200065@std.kitami-it.ac.jp

<sup>6</sup>Member of JSCE, Associate Professor, Faculty of Engineering, Kitami Institute of Technology (ditto)

E-mail: miyamoya@mail.kitami-it.ac.jp

<sup>7</sup>Member of JSCE, Professor, Faculty of Engineering, Kitami Institute of Technology (ditto)

E-mail: kawa@mail.kitami-it.ac.jp

In Japan, great damage to abutment backfills caused by large-scale floods occurs every year. It is necessary to examine the fundamental collapse mechanism on as close to full scale as possible, in order to achieve a sufficient effect of the similarity laws in geotechnical engineering, river engineering, and bridge engineering. In this study, geotechnical evaluations were carried out, such as observation of pore water pressure behavior in an embankment, settlement of an embankment crest, and applicability of a reinforced soil wall as a countermeasure construction, under conditions affected by flowing water. The results show that the collapse behavior of an embankment surface differs depending on the soil properties of the embankment material. The erosion of the river bed progressed even in the footing lower surface of the abutment foundation and in the upstream side of the abutment, where the flow velocity was locally large and changes in the flow direction were confirmed. In addition, when a gabion-reinforced earth wall with water permeability was used for the wall surface construction as a countermeasure, washout of the embankment in the abutment to the extent that a pavement surface above would collapse did not occur, thereby confirming the gabion's usefulness as a countermeasure.

*Key Words* : abutment backfill, flood, gabion-reinforced earth wall, open-channel experiment

## 1. INTRODUCTION

Due to recent global climate change, local and record rainfall has been observed in Japan. **Figure 1** shows the frequency of observations of hourly rainfall,  $r = 50$  mm or more and daily cumulative rainfall,  $R = 200$  mm or more from 1976 to 2019 as observed

by Automatic Meteorological Data Acquisition System (AMeDAS), which is a meteorological observation network of the Japan Meteorological Agency (JMA)<sup>1)</sup>. In this figure, the trend lines drawn by the authors based on JMA data are shown as black lines. Obviously, the numbers of observations with  $r = 50$  mm or more and  $R = 200$  mm or more have increased.

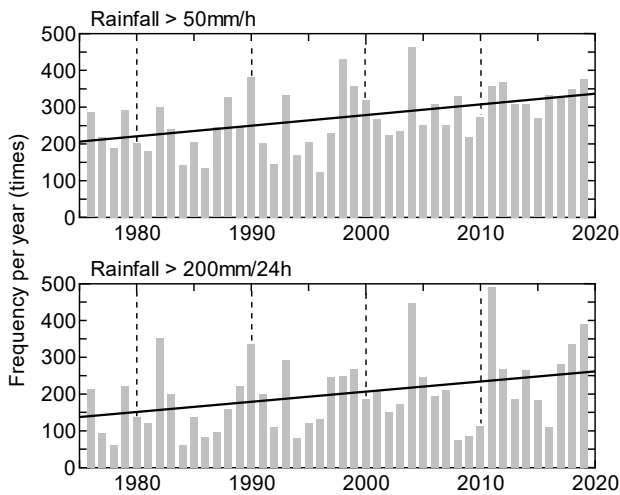
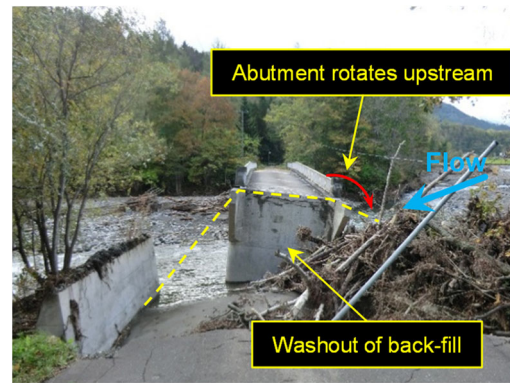


Fig.1 Rainfall trends from 1976 to 2019 (modified JMA<sup>1)</sup>).

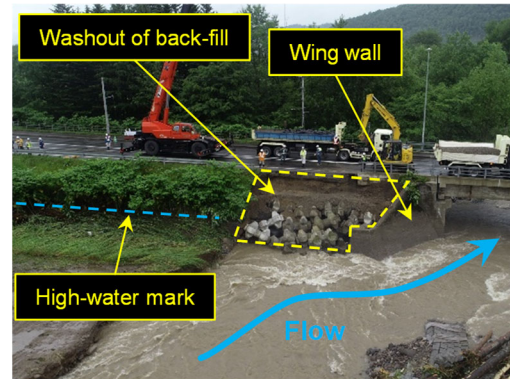
Due to such changes in rainfall and rainfall patterns, large-scale floods cause severe damage to river structures every year in Japan<sup>2), 3), 4)</sup>. Damage in the form of erosion and washout of the abutment backfill is also increasing.

**Figure 2** shows the erosion and washout of the backfill of abutments caused by floods in Japan, as investigated by the authors. **Figure 2(a)** shows the case of the 2016 heavy rainfall disaster in Hokkaido<sup>3)</sup>. Erosion and washout of abutment backfill occurred in Eastern Hokkaido, where record rainfall was observed. A road collapse occurred due to loss of the backfill at the back of the abutment. As a result, a car fell the washout area, causing two human deaths and one missing person. At the spread foundation abutment, the abutment was displaced due to scouring of the foundation ground, and restoring the bridge took time. **Figure 2(b)** shows a case in which abutment backfill flowed out due to record rainfall in the northern Hokkaido area in 2018<sup>5)</sup>. Damage to the abutment backfill affected the transportation of agricultural crops in the farming season. **Figure 2(c)** shows a case of damage by Typhoon No. 19 (Hagibis, SSHWS; Category 5), which caused large-scale damage throughout East Japan in 2019. In this flood, a bridge over the Chikuma River middle basin in Nagano Prefecture suffered a loss of abutment backfill, with three cars falling down and three persons being injured as a result.

In a study on the behavior of abutments and backfill during flooding, as exemplified in **Fig. 2**, Briaud et al.(2009) measured the scour shape around an abutment by a model experiment with different abutment types<sup>6)</sup>. Based on a series of experiments and their analysis, they presented an important report on the prediction method of maximum scouring depth around an abutment. However, the experiment did not simulate erosion and washout of the abutment



(a) Yunosawa bridge, Eastern Hokkaido, 2016.9



(b) Antaroma bridge, Northern Hokkaido, 2018.7



(c) Tanaka bridge, Central Nagano, 2019.9

Fig.2 A typical disaster case in Japan investigated by the authors.

backfill. Also, the river bed material in Briaud's experiment is cohesive soil. In Japan, where there are many river rapids, experimental results on river beds composed of gravel and sand are important. Ettema et al.(2010) conducted an experiment in which the riverbed material was sandy soil, and erosion and washout of the abutment backfill were also reproduced<sup>7)</sup>. The results showed an erosion and flow out at the boundary between the abutment and embankment. However, the foundation of the abutment model was of the pile type, and the behavior of the inclination and displacement of the abutment had not been clarified. Nishimura et al.(2018) conducted an open-channel experiment in a laboratory to reproduce the abutment and backfill damage caused by

large-scale riverbank erosion<sup>8)</sup>. Ishida et al.(2019) studied the applicability of cement-improved soil as a countermeasure against the washout of abutment backfill in flooding by a model experiment<sup>9)</sup>. In addition, the authors conducted an open-channel experiment for a model embankment with a scale ratio of 1/30. Their results showed that erosion progressed from the boundary between the abutment and backfill<sup>10)</sup>. Furthermore, pavement with high rigidity remained in an overhanging state, and a cavity was generated in the road embankment. The study clarified that a reinforced soil wall and slope protection using geosynthetic material were effective countermeasures to prevent such damage.<sup>11)</sup>

The scale model experiment with the laboratory open-channel shown above shows useful experimental results as benchmarks on erosion and washout of abutment backfill due to floods. However, small-scale experiments make it difficult for geotechnical engineering, river engineering, and bridge engineering to satisfy the relevant similarity laws. In particular, the displacement of an abutment becomes a problem in view of the bearing capacity of the foundation ground, the hydrodynamic force of river water, and the weight of the abutment including girders, and this is difficult to reproduce sufficiently in a small-scale model. The various forms of flood damage that have occurred in Japan in recent years, such as those caused by the heavy rainfall in western Japan in 2018 and typhoon No. 19 that occurred in Japan, are extensive in terms of the affected areas, and officials are required to quickly judge the soundness of bridge facilities and to resume their use as transportation routes as soon as possible. In other words, there is an urgent need to establish a method for assessing the remaining bearing capacity of bridge piers and abutments and the soundness of structural members after a flood. Therefore, it is necessary to understand the basic behavior by experiments at full-scale or as close to full-scale as possible, in which the effects of the similarity laws of geotechnical engineering, river engineering, and bridge engineering are sufficiently exerted.

This study reproduced abutment backfill in a state close to full-scale using a large-scale open-channel at the research facilities of Kitami Institute of Technology. The Institute reproduced a river with a scale ratio of 1/5, and attempted detailed observations of the erosion and washout mechanism in a flood and the inclination process of an abutment. In addition, to study the countermeasures, a model of a gabion-reinforced soil wall composed of a crushed stone-filled gabion and reinforcements was prepared, and an effect verification experiment was conducted. This paper presents geotechnical evaluations such as pore

water pressure behavior in the embankment, settlement at the crown of the embankment, and applicability of the gabion-reinforced soil wall as countermeasures work under flood conditions.

## 2. TEST PROGRAM

### (1) Open-channel apparatus

**Figure 3** shows an overview of the large-scale open-channel apparatus used in this study. The water channel length is 70 m, and water reservoir tanks are provided at the upstream and downstream ends of this water channel. The slope of the riverbed is 1/100. Water was flooded into this reservoir before the experiment, and the water was circulated in the channel by a pump installed in the downstream reservoir. **Figure 4** shows the grain-size distribution of the geomaterial in this study. Within the range of 15m upstream and downstream from the central part of the open-channel, gravelly sand (SG, Maximum grain size,  $D_{\max} = 26.5$  mm, Average grain size,  $D_{50} = 0.44$  mm, Fine fraction content,  $F_c = 8.1\%$ ) was deposited up to 0.8 m from the riverbed. In the area, 10 m upstream and downstream of the SG area, soil classified as fine-grained gravel sand (SFG,  $D_{\max} = 26.5$ mm,  $D_{50} = 0.25$ mm,  $F_c = 38.6\%$ ) was cut to form an open-channel. In the area of 10 m near the reservoir tank, protection works were placed on the riverbed and riverbank for the purpose of rectifying the flow of river water. The target of the experiment in this study was a situation where frontal flow acts on the backfill of an abutment of a small bridge in an area without an embankment in the upstream area of small- and medium-sized rivers such as those shown in **Fig. 2(a)** and **Fig. 2(b)**. Note that, the geomaterial was selected so that the required amount could be secured in three large-scale experiments. In addition, in this study, the erosion rate and hydraulic conductivity were unknown because the geological materials were not investigated using the EFA (Erosion Function Apparatus)<sup>12)</sup> or the hydraulic permeability test.

### (2) Experiment conditions

In this research, the abutment and backfill installed in the river were reproduced by a model with a scale ratio of 1/5. As the simplest river condition, a model embankment was installed in the open-channel assuming that the front flow acts on the embankment slope and the abutment side. In the experiment, three cases were examined in which the river width, the soil quality of the embankment material used for the model embankment, and the condition of countermeasure work were changed. Case-1 is a basic experiment case where the river width is 1.3 m and the embankment material is sandy soil. In Case-2, the river

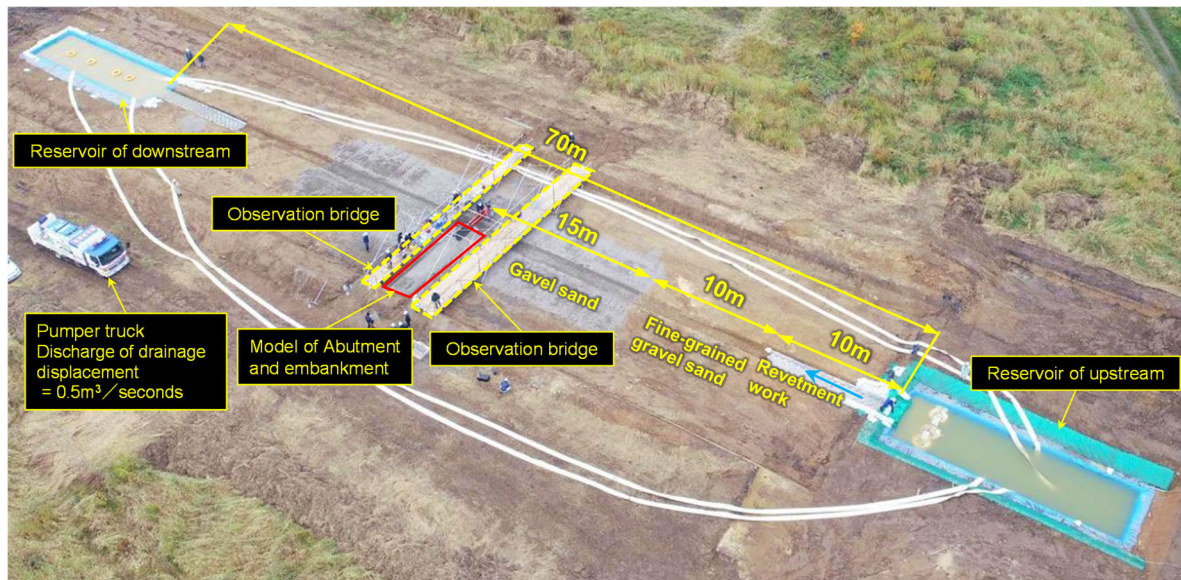


Fig.3 Overview of open-channel apparatus.

Table 1 Target of hydraulic conditions.

Case	Flow rate, $Q$ (m <sup>3</sup> /s)	River level, $H_r$ (m)	Flow velocity, $U_w$ (m/s)
1, 2	0.34	0.25	1.08
3	0.89	0.25	1.20

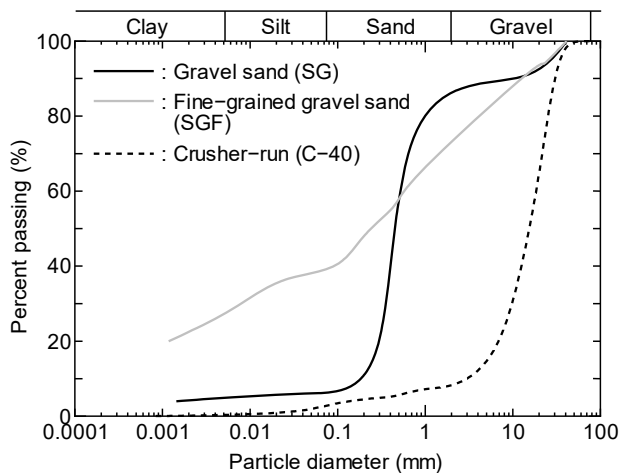


Fig. 4 Grain size distributions.

width was made 3.3 m to observe the effect of river meandering, and fine-grained gravel sand was used as the embankment material. In Case-3, the river width and embankment material are the same as in Case-1, and a gabion-reinforced earth wall was installed upstream of the embankment to verify the effect of countermeasures. **Table 1** shows the hydraulic conditions set as the target values in this experiment. The flow rate  $Q$ , was set so that the river level  $H_r$ , was 0.25 m in each case. The flow velocity  $U_w$ , calculated by Manning's formula with Manning's coefficient of roughness set to 0.03<sup>13)</sup> and the riverbed set to 1/100 is 1.08m/s for Case-1 and Case-2, and 1.20m/s for Case-3. The river surface velocity distribution obtained from the PIV analysis in Case-3 as shown in **Fig. 18** will be described later. It should be noted that the results of the PIV analysis are reference values

because the river surface velocity and river width are widening, but the  $U_w$ , excluding the local flow around the the abutment, is about 1.0 ~ 1.2 m/s. From this result, it seems that the target flow velocity calculated from Manning's formula shown in **Table 1** is generated in the experiment. The pumper trucks used were one vehicle for Case-1 and Case-2, and two vehicles for Case-3. However, in the experiment, it was difficult to keep  $H_r = 0.25$ m constant because pumper truck and hose loss and leakage, bank erosion, and riverbed degradation occurred. A future task of this study is to keep the water level such as the flow rate constant.

The similarity law uses the Froude similarity law in hydraulic engineering, and  $Q$  and  $H_r$  of the experimental model are set so that  $U_w$  on the prototype scale is 2 - 3 m/s<sup>14), 15)</sup> when the scale ratio is 1/5.

**Figure 5** shows an outline of the model embankment of Case-1. **Figure 6** shows the state of the model embankment before the experiment of Case-1, taken from the right bank. Case-1, with an open-channel length of 70m, width of 1.3m, and depth of 0.3m, shows the basic experimental case. Therefore, protection works to prevent erosion are not carried out on the river bank. In all experimental cases, asphalt pavement was laid on top of the embankment. Note that the pavement thickness is 30 mm. At the points shown in **Figure 5**, three undisturbed specimens were sampled using a soil sampler (diameter 50 mm, height 51 mm). The average values of dry density,  $\rho_d$  and water content,  $w$ , were  $\rho_d = 1.46$ g/cm<sup>3</sup> and  $w = 5.0$ %.

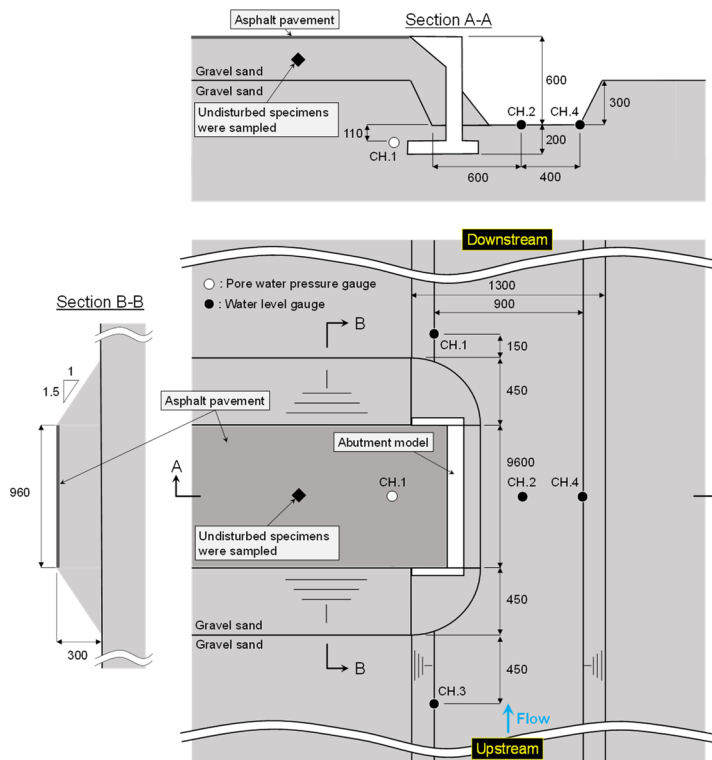


Fig.5 Experiment condition of Case-1.

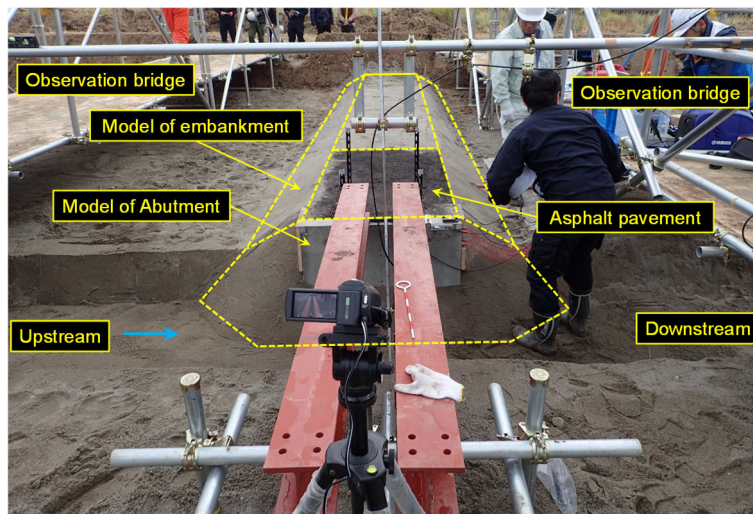


Fig.6 Model embankment and abutment of Case-1 (Photo taken from the right bank).

Figure 7 shows an outline of the Case-2 model embankment. Figure 8 shows the state of the model embankment before the experiment of Case-2, photographed from the upstream side of the left bank. In Case-2, the length of the open-channel was 70m, the width was 3.3m, and the depth was 0.3m; the river was widened to reproduce the meandering of a river. In addition, Case-2 aims to evaluate the influence of the soil quality of the backfill on erosion and wash-out. Therefore, unlike the soil material used in Case-1, fine-grained and gravelly sand, which is similar to the ground of the open-channel, was used as the embankment material. In Case-2, a backfill was constructed on the right bank using gravel sand as the

embankment material. At the points shown in Fig. 7, The average  $\rho_d$  and  $w$  measured by the same method as Case-1 were  $\rho_d = 1.34\text{g/cm}^3$  and  $w = 26.8\%$ .

Figure 9 shows an outline of the Case-3 model embankment. In Case-3, the purpose was to observe the effect of the countermeasure method at high water level. Therefore, in order to prevent the river water level from decreasing due to bank erosion, a protection work was installed on the river bank using concrete blocks and non-woven fabric. No protection work was installed in the area 1 m downstream from the countermeasure construction. In Case-3, the dry density and water content were not measured. However, the same embankment material as the one used

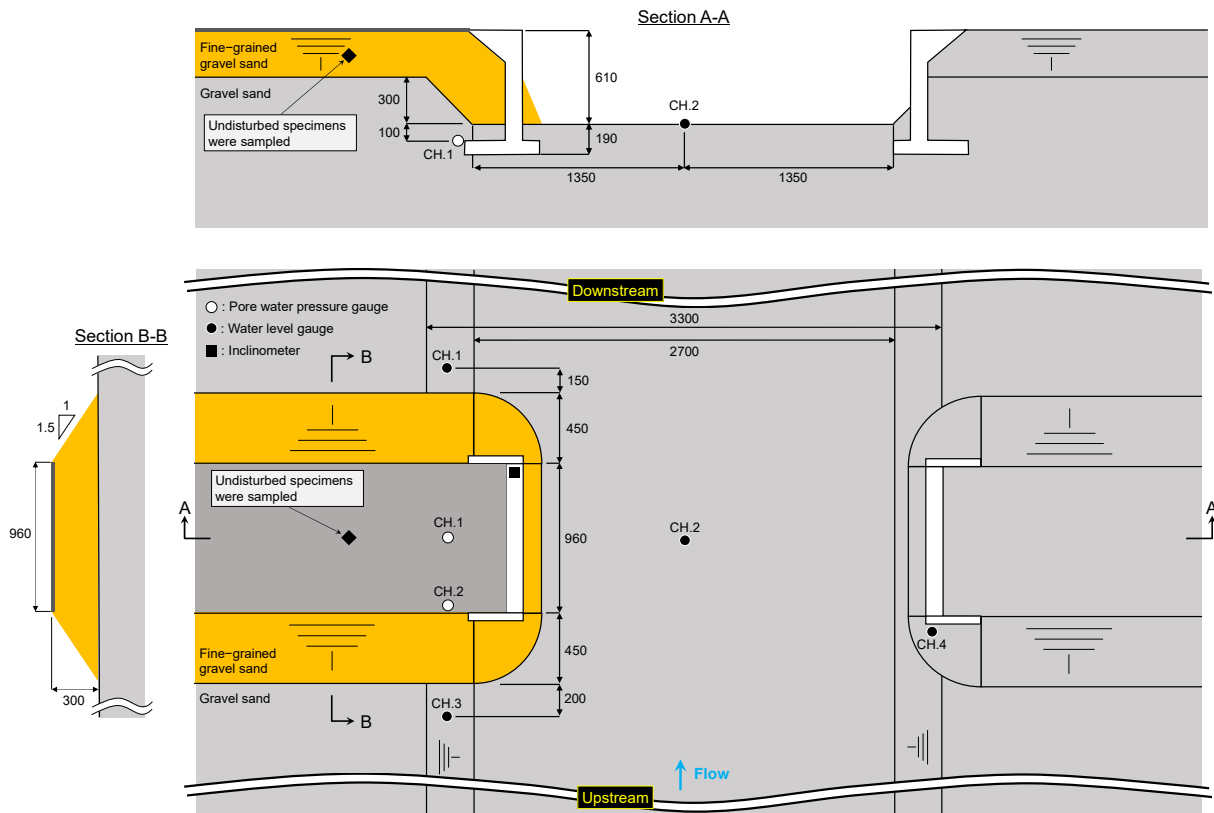


Fig.7 Experiment condition of Case-2.

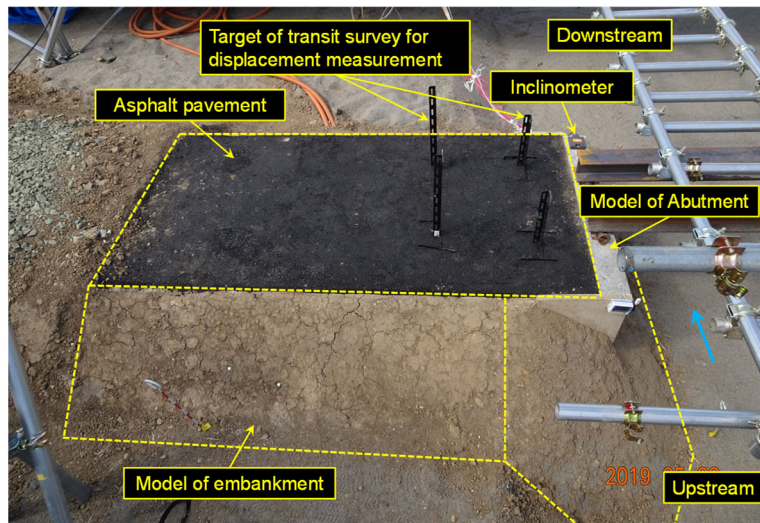


Fig. 8 Model embankment and abutment of Case-2 (Photo taken from the light bank, upstream).

in Case-1 was prepared by the same method and an embankment was constructed. Therefore,  $\rho_a$  and  $w$  are expected to be similar to Case-1.

Figure 10 shows production underway on the model of the gabion-reinforced soil wall used as the countermeasure method installed in Case-3. Here, the gabion-reinforced soil wall uses a gabion with a height of 1 m, a width of 1 m, and a length of 2m shown in Fig. 11(a) as wall material. The gabion-reinforced earth wall uses hexagonal wire mesh with a length of about 2 m that is integrated with this wall material as a reinforcement (see Fig. 11(b))<sup>16), 17)</sup>.

In this test, as a unit of the gabion-reinforced earth wall model, a wall cage made of hexagonal wire mesh with a height of 0.2m, depth of 0.2m, and length of 0.4m was used as the wall material. A 0.3m-long tortoise wire mesh reinforcement was attached to the wall material. A gabion-reinforced clay wall model was installed with three units in the height direction, two units in the road extension direction, and one unit in the road crossing direction. Triangular prismatic gabion-reinforced soil was prepared and installed at the corners. In addition, one unit (height 0.2m) was buried under the riverbed. Also, non-woven fabric

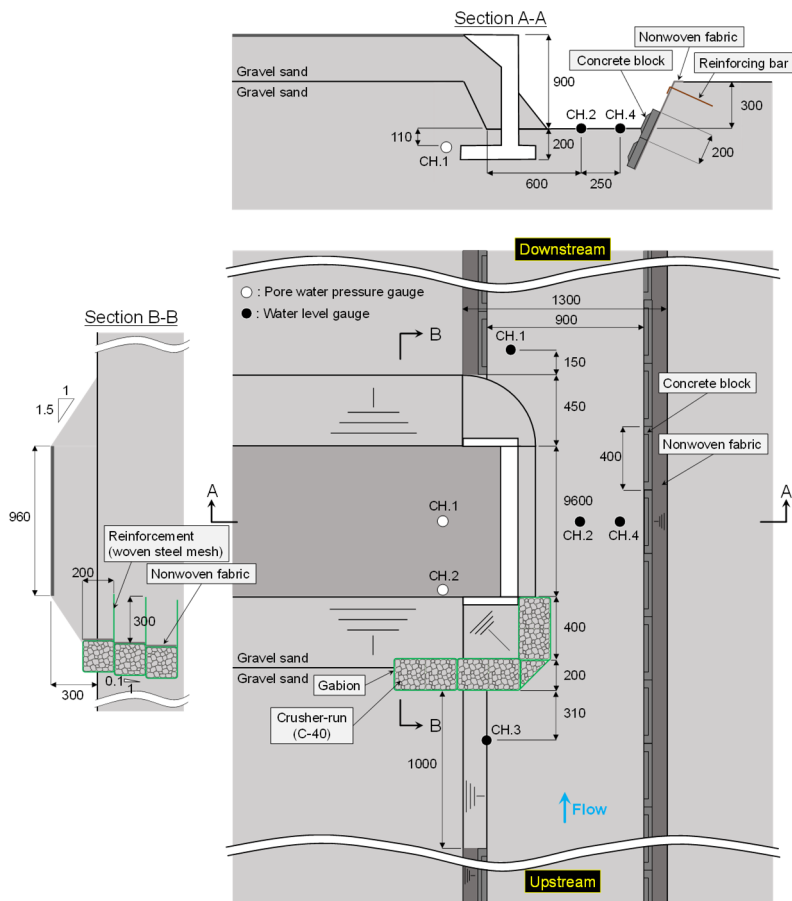


Fig.9 Experiment condition of Case-3.



Fig.10 Construction process of model gabion-reinforced soil wall.

was placed at the boundary between the gabion-reinforced soil wall and backfill soil on each level. As for the geomaterial in the gabion, full-size cobblestone (particle size was 100 ~ 250mm)<sup>16), 17)</sup> was used. Therefore, Crusher run (C-40,  $D_{max} = 37.5\text{mm}$ ,  $D_{50} = 15.4\text{mm}$ ,  $F_c = 2.5\%$ , see Fig.4) was adopted for the gabion-reinforced earth wall model.

Figure 12 shows the model abutments used in all experimental cases. The model abutment is a reinforced concrete structure of the footing foundation type with a height of 0.8m and a width of 0.96m. According to a field survey shown in Fig. 2, many of the damaged abutments had no sidewalls, but small wing walls were attached. This model abutment was intentionally set to a large blockage rate by projecting 0.2m in Case-1 and Case-3 and 0.3m in Case-2. This experimental state reproduces the condition before the river flow inhibition rate was severely limited. The measurement items under experiment are pore water pressure in the model embankment measured by a pore water pressure gauge, river water level in the river channel measured by a water level gauge, and displacement of the model embankment crest as determined by surveying.

Since the slope of the abutment due to scouring of the abutment foundation ground was anticipated in

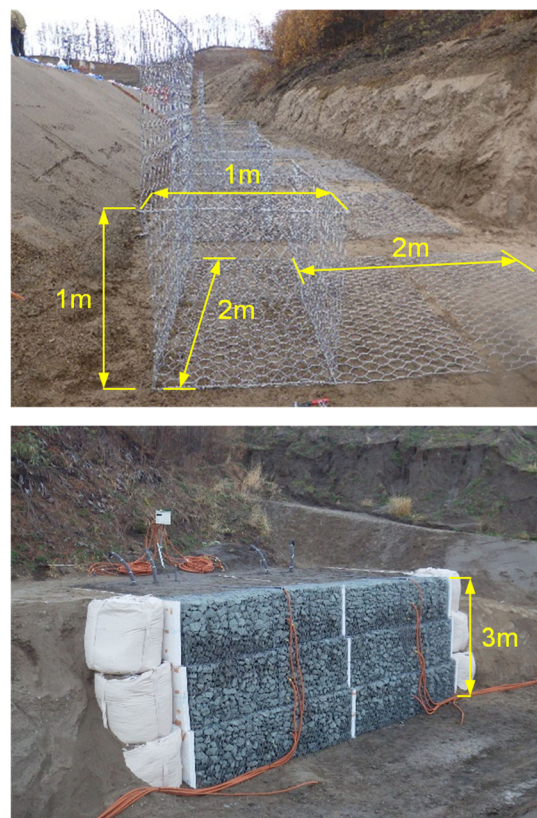


Fig.11 Full-scale gabion-reinforced earth wall<sup>16), 17)</sup>.

Case-2 where the river area inhibition rate was large, an inclinometer and a fixed PIV (Particle Image Velocimetry) camera were installed to observe the flow state around the abutment.

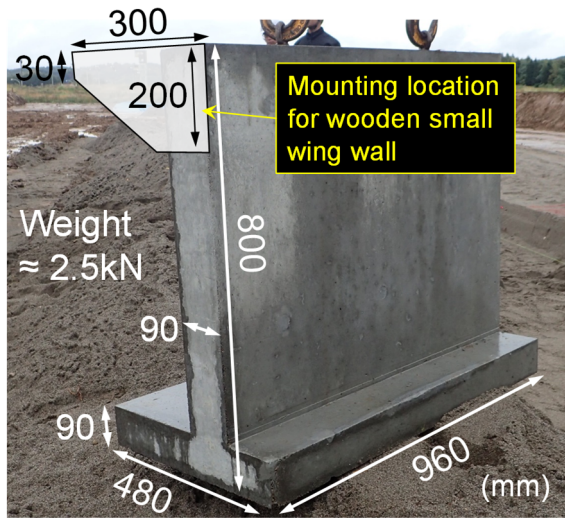


Fig.12 Overview of the model abutment.

### 3. TESTS RESULTS AND DISCUSSION

#### (1) Overview of collapse process

Figures 13(a), 13(b), and 13(c) show the situation of the model embankment during the experiments in Cases-1, 2, and 3, respectively.

In Case-1, which used sandy soil as the embankment material, the river surface reached the model embankment slope on the upstream side immediately after it was eroded and washed away by the embankment slope and the front abutment wall. After that, erosion progressed from the boundary between the model embankment and the abutment model to the inside of the embankment. Eventually, a tunnel-shaped cavity from upstream to downstream was generated in the backfill of the abutment. Then, at the elapsed time  $t = 134$  minutes, the paved surface, which had lost bearing capacity, completely collapsed. This result is similar to those of Ettema et al.<sup>7)</sup>, Nishimura et al.<sup>4)</sup>, and Kawajiri et al.<sup>10)</sup>, who conducted scale model experiments using sandy soil.

Next, in Case-2, which used fine-grained and

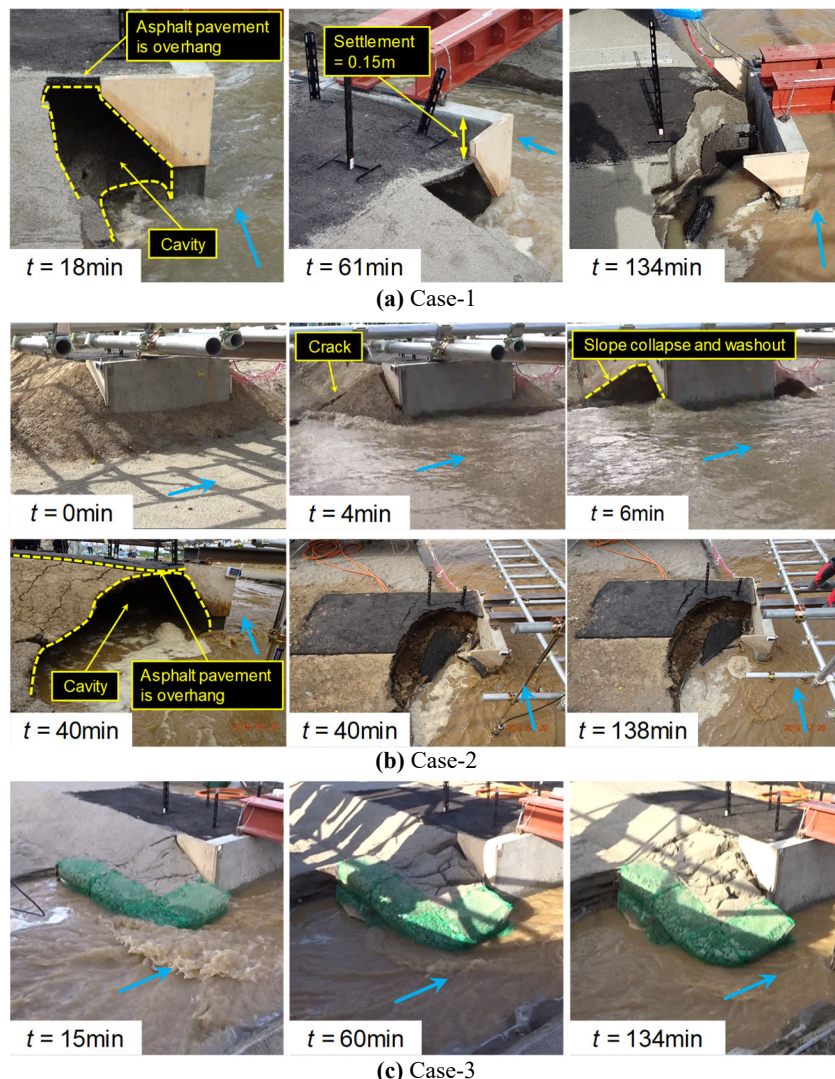


Fig.13 Change to embankments and abutments during the experiment.

gravel sand as the embankment material, a crack occurred on the upstream slope at  $t = 4$  minutes, and the upstream slope of the embankment collapsed due to clods and was washed away. After that, erosion and outflow proceeded from this collapse surface; the paved surface was in an overhanging state 40 minutes after the start of the experiment; and the paved surface that had lost bearing capacity collapsed at  $t = 44$  minutes. Case-2, which used fine-grained and gravelly sand, had a higher fine-grained content compared to Case-1, so the slope erosion resistance due to running water was high on the embankment-supporting ground, which was gravel-sand. It is thought that the embankment slope, which lost bearing capacity due to local scouring and the outflow of supporting ground, suddenly collapsed.

This result confirms that it is necessary to consider the material of the embankment and the soil property of the supporting ground as a flood countermeasure in the large-scale experiment of this study. In this study, the effectiveness of the measures against the gabion-reinforced soil wall shown in Fig. 15 was verified by a large-scale experiment.

Figure 15 shows the concept of the abutment backfill with gabion-reinforced soil walls as a countermeasure against flood. A gabion made with cobblestone as filling material is used as the wall material. As a result, river water flows into the gabion, but it is possible that the fluid force that erodes the embankment can be reduced by decreasing the flow velocity. In addition, since the buried part in the riverbed allows the running water inside the riverbed to flow smoothly downstream, it reduces the sudden scouring and destabilization of the front of the revetment and the foundation that occur during conventional concrete protection work. The gabion-reinforced soil wall can be expected to behave as a reinforced soil wall using woven steel mesh. Furthermore, since the wall material is composed of cobblestone, it can be inferred that the water level in the abutment backfill decreases rapidly after the river water level decreases, which contributes to the stability of the embankment. When the foundation of the gabion-reinforced soil wall is scoured, the backfill soil, which functions as a reinforcement soil wall, does not suddenly flow out, and settlement is suppressed. As a result, its performance as a transportation geotechnical structure can be secured even during floods.

Figure 13(c) shows the model embankment in the experiment photographed from the upstream side in Case-3. When a gabion-reinforced soil wall was used as a countermeasure, riverbed scouring proceeded at the corner of the installation site, and the part in front of the reinforced soil wall model settled. However,

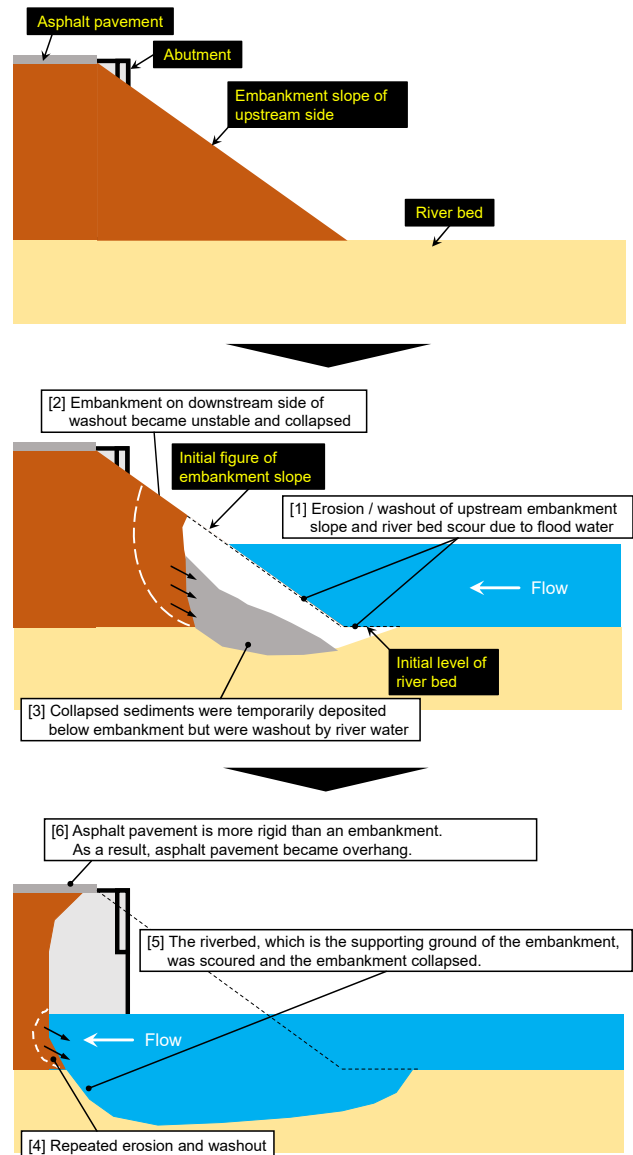


Fig.14 Estimation mechanism of embankments and abutments by flood.

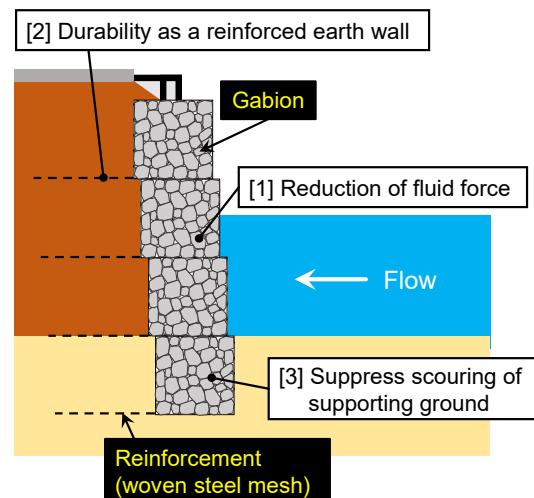


Fig.15 Concept for countermeasure work of embankments and abutments against flood.

washout of the backfill was suppressed, and no cavity was formed under the pavement. In other words, the damage to the pavement surface could be reduced.

## (2) Time history of measurement values

**Figure 16** shows the changes in the measured values of Case-1. In Case-1, riverbank erosion occurred and river width widened due to an increase in flow rate corresponding to a gradual rise of river water level. Therefore, the river water level  $H_r$  was about  $H_r = 180\text{mm}$ . As  $H_r$  rises, the pore water pressure converted into the pressure head  $h_w$  in the embankment ( $h_w = 0\text{mm}$  at the top of the footing) rises. As for the vertical displacement,  $d_v$  of the pavement surface (settlement is +), settlement of  $d_v = 3\text{mm}$  occurred at the upstream measurement point ( $\square$  in the figure) at the back of the abutment. At  $t = 50$  minutes, settlement proceeded rapidly until measurement by transit survey became impossible. As a result, the road cave-in shown in **Fig. 13(a)** occurred. The same tendency is observed at the downstream measurement point ( $\triangle$  in the figure) at the back of the abutment. However, no significant relationship can be confirmed between the progress of road cave-in caused by the progress of such slope erosion and the change in pore water pressure (pressure head) at the center of the embankment. Therefore, the erosion and outflow of the backfill are dominated by the influence of erosion and scouring by the direct action of river water on the embankment slope rather than the fluctuation of the water level inside the embankment. Note that no significant displacement occurred on the abutment according to the results of a survey on the abutment after the experiment.

**Figure 17** shows the changes in the measured values in Case-2. In Case-2, the results of the inclinometer installed on the abutment are also shown. In Case-2, a large flow was able to flow by expanding the river width from 1.3m to 3.3m.  $H_r$  was locally low in some areas, but the maximum was about  $H_r = 280\text{mm}$  until  $t = 30$  minutes. After  $t = 30$  minutes,  $H_r$  gradually decreased as the river bed scour progressed. As described above, in Case-2, the upstream slope collapsed all at once, so that the measurement points ( $\square$  and  $\circ$ ) on the upstream side of  $d_v$  could not be measured by surveying by  $t = 50$  minutes. Then, settlement of the pavement on the downstream side progressed. That is, in Case-2, settlement occurred in a wide area at the backfill crown of the abutment. This tendency is different from Case-1.

$h_w$  tends to rise faster at CH.2 installed on the lower slope of the upstream side. However, similar to Case-1, in the central part of the embankment (CH.1) and the lower part of the slope (CH.2), no significant relationship can be confirmed between the increase and decrease of  $h_w$  and the collapse behavior of the

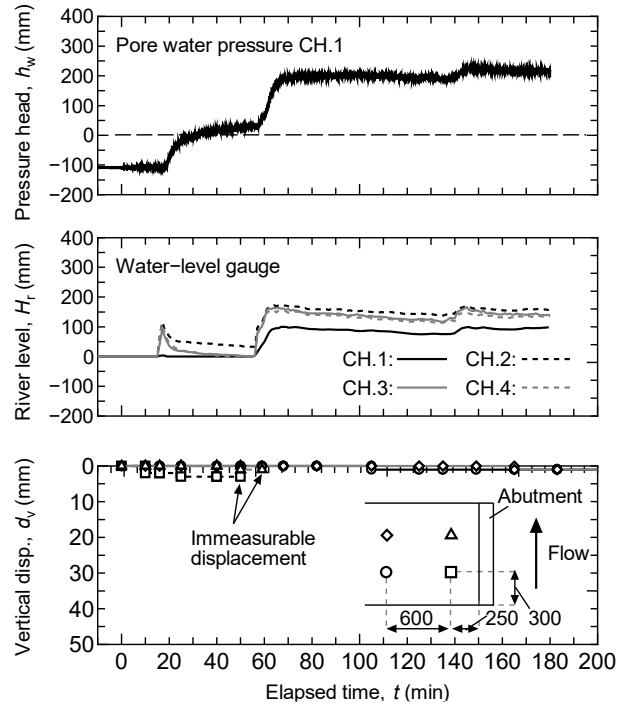


**Fig.16** Changes in measured values in Case-1.

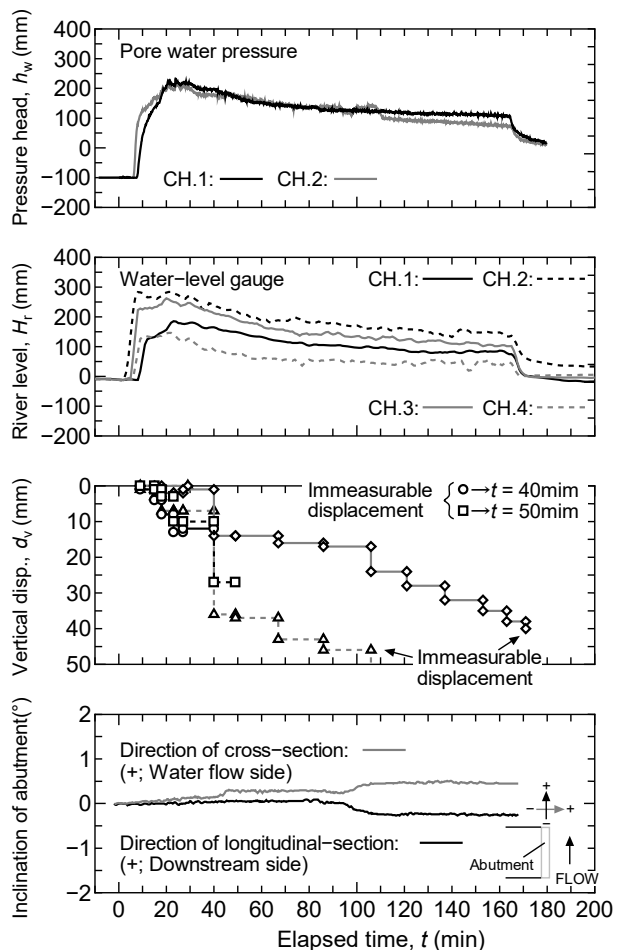


**Fig.17** Changes in measured values in Case-2.

abutment backfill.

The inclination of the abutment increased in the river directly from  $t = 20$  minutes after  $d_v = 10\text{mm}$ .

At  $t = 95$  minutes, the slope to the river and the slope to the upstream increased rapidly. At this time,  $h_w$  rises slightly. This can be expected, because the scour of the ground around the pore water pressure gauge progressed and the position of the pore water pressure gauge moved downward. Therefore, it can be inferred that the scouring of the foundation ground near the abutment footing proceeded after  $t = 20$  minutes.

**Figure 18** shows a typical result of the velocity distribution around the abutment upstream obtained

from the PIV analysis. At  $t = 40$  minutes, the flow velocity locally increased on the upstream side of the abutment, and at  $t = 92$  minutes, the flow direction was turning around at the back of the abutment. Such a change in the local flow around an abutment is considered to affect the external force on the inclination of the abutment during a flood. As described above, in Case-2, the upstream slope suddenly collapsed, and the measurement points ( $\square$  and  $\circ$ ) on the upstream side of  $dv$  could not be measured by  $t = 50$

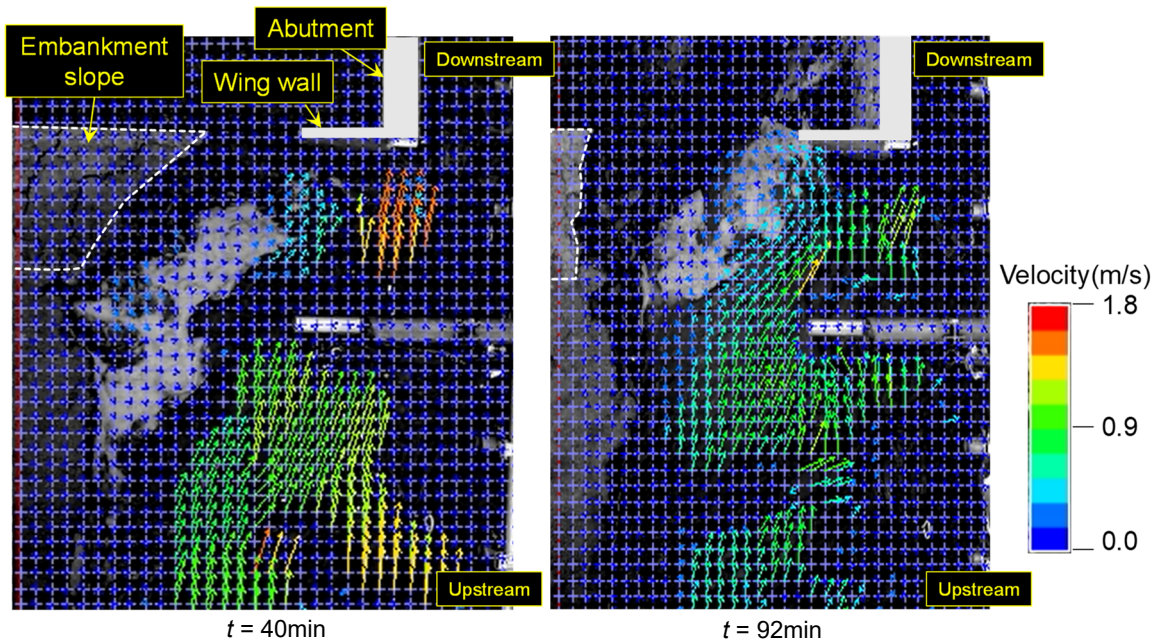


**Fig.18** Results of PIV analyse in Case-2.

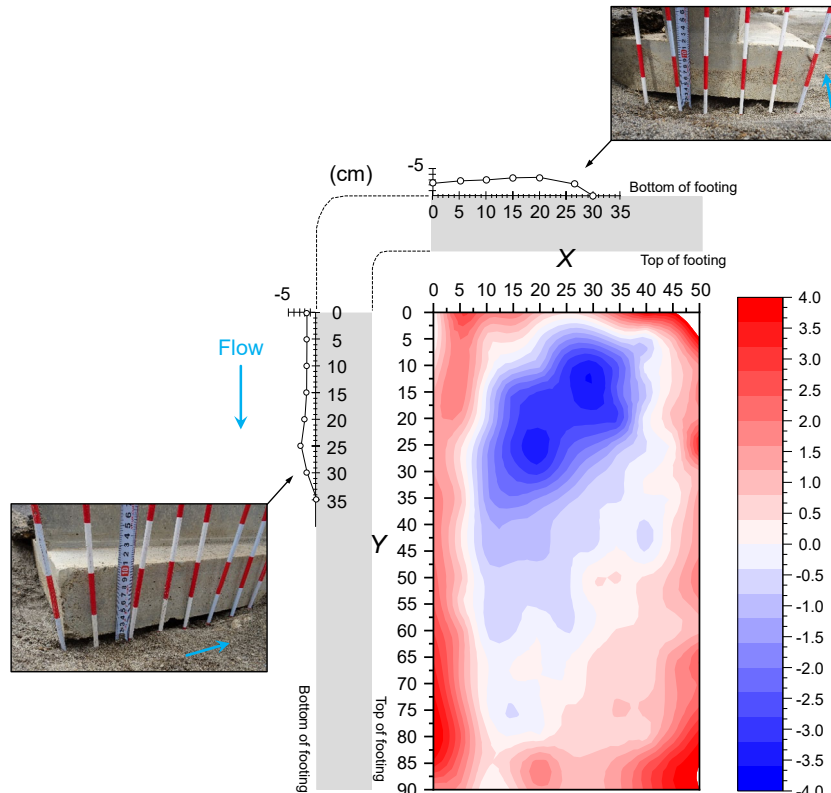


**Fig.19** Result of scour depth after experiment in Case-2.

minutes. Then, settlement of the pavement on the downstream side progressed.

**Figure 19** shows the scouring depth in the footing bottom ground of the left bank abutment after the test. In the figure, the apparent scouring depth measured from the exposed footing end face is measured and shown as a line graph. After measuring the external scouring depth, the abutment was carefully lifted by a crane and removed. After that, a 5cm mesh was created on the bottom surface of the footing, and the scouring depth at the intersection of the meshes was measured and expressed as a contour diagram. In this contour diagram, the flattest point in the measured values was the scouring depth of 0cm. The apparent footing scouring that can be seen occurred on the upstream riverside, and the scouring depth was about 4 cm at maximum on the upstream footing end face. Next, regarding the scouring depth of the bottom surface of the footing, since the riverbed around the footing collapsed when the abutment was lifted, sediment had accumulated at the outer edge of the footing. However, the scouring depth is large in the area of the bottom surface of the footing ( $X = 15$  to  $30$ cm,  $Y = 20$  to  $30$ cm) on the extension line where the amount of scour on the exterior is large, and is about 4 cm at maximum. This scouring depth agrees with the apparent scouring depth measured, and from this, it can be expected that a cavity of up to about 4cm was formed upstream of the abutment footing underside of the river. This result confirms that the abutment inclination occurred upstream on the riverside.

**Figure 20** shows the changes in the measured values in Case-3. In Case-3, the river water level was about  $H_r = 270$ mm, because the bank was constructed to prevent riverbank erosion. The river water level was higher than in Case-1 having the same river width. After observing the maximum value of  $H_r$ , bed scour progressed rapidly and  $H_r$  decreased sharply. In addition, the maximum value of  $h_w$  is lower than in Case-1 and Case-2, which have no countermeasures. The vertical displacement at the crown of the embankment is about  $d_v = 1.3$ mm and settlement has not progressed.

Therefore, a gabion-reinforced earth wall reduces the inflow and erosion of river water into a back abutment embankment and can suppress destabilization of abutment backfill during a flood.

#### 4. CONCLUSIONS

In this study, a large-scale open-channel experiment was carried out to demonstrate the erosion and washout mechanism of abutment backfill, which has frequently occurred in recent floods in Japan, and to

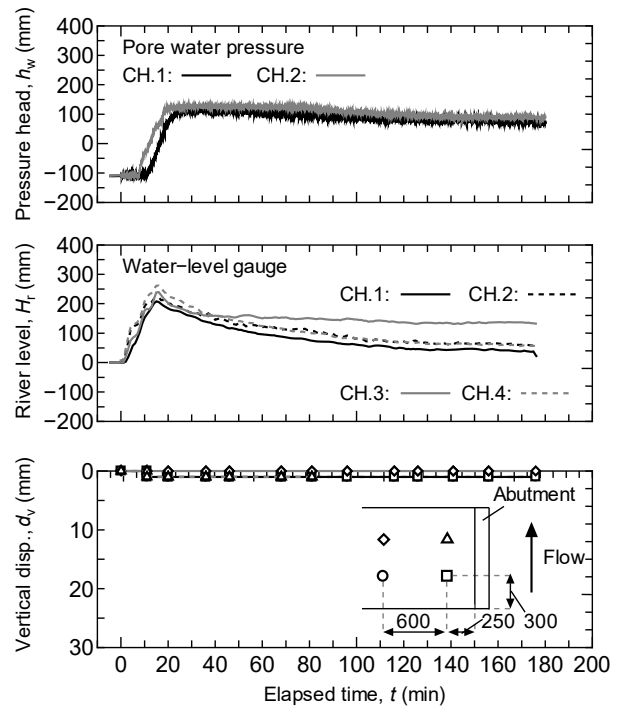


**Fig.20** Changes of measured values in Case-3.

propose its countermeasure construction. The following findings were obtained.

- 1) When gravel sand was used as the embankment material, embankment erosion progressed at the structure boundary with the abutment, and erosion and loss of embankment in the abutment were remarkable. In addition, an overhang was caused in the pavement surface in the upper part where the embankment flowed out.
- 2) When fine-grained gravel sand was used as the embankment material, the upstream side slope, which lost its bearing capacity due to erosion of the river bed, collapsed immediately after cracking occurred. Erosion and washout continued afterwards, and a part of the pavement surface collapsed.
- 3) The erosion of the riverbed progressed on the bottom surface of the footing, and abutment inclination was generated upstream of the river side due to the locally high flow velocity and the change in flow direction on the upstream side.
- 4) The gabion-reinforced soil wall, which had water permeability on the wall, was partially deformed by the flood. However, the outflow of embankment in the abutment, which would otherwise cause the pavement to collapse, did not occur, thereby confirming the gabion's usefulness as a countermeasure work.

Small-scale open-channel experiments to date have also provided similar qualitative data as shown above<sup>10), 11)</sup>. However, the results of this large-scale

experiment showed quantitative data, such as the amount of scouring around the abutment foundation, the inclination angle of the abutment, and the effect of the reinforcing material, which are difficult to measure by the scale effect in a small model experiment. In other words, this result is useful data for planning concrete countermeasures in the future. In the future, it will be necessary to apply the bed load similarity law in order to understand the more detailed collapse mechanism.

**ACKNOWLEDGMENTS:** The authors would like to acknowledge the research grant from KAKENHI (17K17571) and the River Center of HOKKAIDO, RIC. The authors also appreciate the very kind support of Mr. Inoue of Hokkaisuiko Consultant Corporation Co., Ltd., and Hokkaido Regional Development Bureau, Ministry of Land, Infrastructure, Transport and Tourism (MLIT), which cooperated greatly in the experiment.

## REFERENCES

- 1) Japan Meteorological Agency [https://www.data.jma.go.jp/cpdinfo/extreme/extreme\\_p.html](https://www.data.jma.go.jp/cpdinfo/extreme/extreme_p.html) (in Japanese) (refer 4/15/2020)
- 2) Yasuda, S., Shimizu, Y. and Deguchi, K.: Investigation of the mechanism of the 2015 failure of a dike on Kinu river, *Soils and Foundations*, Vol. 56, No. 4, pp. 581–592, 2016.
- 3) Kawajiri, S., Kawaguchi, T., Watanabe, Y., Hayakawa, H., Miyamori, Y., Nakamura, D. and Yamashita, S.: Investigation report of geotechnical disaster on river area due to typhoon landfall three times on Okhotsk region, Hokkaido, Japan, *Soils and Foundations*, Vol. 59, No. 3, pp. 764-782, 2019.
- 4) Nishimura, S., Takeshita, Y., Nishiyama, S., Suzuki, S., Shibata, S., Shuku, S., Komatsu, M. and Kim, B.: Disaster report of 2018 July heavy rain for geo-structures and slopes in Okayama, *Soils and Foundations*, Vol. 60, No. 1, pp. 300-314, 2020.
- 5) Kawajiri, S., Watanabe, Y., Matsuda, T., Onmayashiki, K. and Miyamori, Y.: Investigating report of river structure damage at northern and eastern Hokkaido due to heavy rainfall, July 2019, *Advances in River Engineering*, Vol. 25, pp. 85-90, 2019. (in Japanese)
- 6) Briaud, J.-L., Chen, H.-C., Chang, K.-A., Oh, S. J. and Chen, X.: Abutment scour in cohesive materials, NCHRP Report 24-15(2), National Research Council: *Transportation Research Board*, 2009.
- 7) Ettema, R., Nakato, T. and Muste, M.: Estimation of scour depth at bridge abutments, NCHRP Report 24-20, National Research Council: *Transportation Research Board*, 2010.
- 8) Nishimura, Y., Takeuchi, Y. and Suwa, Y.: Experimental study on the basic mechanism of abutment damage caused from large-scale bank erosion, *Advances in River Engineering*, Vol. 24, pp. 149-154, 2018. (in Japanese)
- 9) Ishida, Y., Takayama, S., Izuno, K., Satofuka, Y., Kobayashi T. and Fukagawa, R.: Prevention of soil outflow from the ground around bridge abutment using cement soil stabilization, *International Journal of GEOMATE: Geotechnique, Construction Materials and Environment*, Vol. 19, No. 71, 2020.
- 10) Kawajiri, S., Kawaguchi, T., Watanabe, T., Miyamori, Y., Kawamata, S., Onmayashiki, K., Kaneko, T. and Takahashi, H.: Geotechnical properties and observation of erosion process by hydraulic model test of backfill of abutment, *Journal of Japan Society of Civil Engineers B1*, Vol. 74, No. 4, pp. I\_1273-1278, 2018. (in Japanese)
- 11) Kawajiri, S., Onmayashiki, K., Kawaguchi, T., Kurachi, S. and Harata, M.: Proposal for countermeasure by using geosynthetics against erosion for backfill of abutment due to flooding, *Geosynthetics Engineering Journal*, Vol. 33, pp. 159-166, 2018. (in Japanese)
- 12) Karim, Md. Z. and Tucker-Kulesza, S. E.: Predicting soil erodibility using electrical resistivity tomography, *Journal of Geotechnical and Geoenvironmental Engineering*, Vol. 144, No. 4, 2018.
- 13) Phillips, J. V. and Tadayon, S.: Selection of Manning's roughness coefficient for natural and constructed vegetated and non-vegetated channels, and vegetation maintenance plan guidelines for vegetated channels in Central Arizona, *USGS Scientific Investigations Report*, 2006 - 5108, 2006.
- 14) Fujita, I.: Development and application of image analysis software KU-STIV for river surface flow measurements, *Memoirs of Construction Engineering Research Institute*, Vol. 57, pp. 81-92, 2015. (in Japanese)
- 15) Yorozuya, A., Motonaga, Y. and Iwami, Y.: Technique of water & sediment flow measurement of rivers during flooding, *NAGARE*, Vol. 32, pp. 359-364, 2013. (in Japanese)
- 16) Kawamata, S., Kawaguchi, T., Nakamura, D., Kurachi, Y., Hayashi, K., Kawajiri, S. and Yamashita, S.: Performance evaluation for gabion faced reinforced soil wall in a cold, snowy environment using permeable heat insulating materials, *Geosynthetics Engineering Journal*, Vol. 31, pp. 119-126, 2016. (in Japanese)
- 17) Kawamata, S., Kurachi, Y., Kawaguchi, T., Kawajiri, S., Nakamura, D., Yamashita, S. and Hayashi, K.: Moisture behavior on gabion faced reinforced soil wall in cold, snowy environment, *Proceedings of the 11th International Conference on Geosynthetics*, 2018.

(Received July 7, 2020)  
(Accepted January 30, 2021)